

See discussions, stats, and author profiles for this publication at: <https://www.researchgate.net/publication/341779038>

Lane Detection: A Survey with New Results

Article in Journal of Computer Science and Technology · May 2020

DOI: 10.1007/s11390-020-0476-4

CITATIONS

7

READS

4,360

5 authors, including:



Yuanchen Guo

Tsinghua University

11 PUBLICATIONS 9 CITATIONS

SEE PROFILE



Shao-Kui Zhang

Tsinghua University

10 PUBLICATIONS 36 CITATIONS

SEE PROFILE

Journal of Computer Science & Technology



SPONSORED BY INSTITUTE OF COMPUTING TECHNOLOGY
THE CHINESE ACADEMY OF SCIENCES &



CHINA COMPUTER FEDERATION



SUPPORTED BY NSFC



CO-PUBLISHED BY SCIENCE PRESS &

Lane Detection: A Survey with New Results

Dun Liang¹, Yuan-Chen Guo¹, Shao-Kui Zhang¹, Tai-Jiang Mu^{1,*}, Member, CCF, and Xiaolei Huang²

¹Department of Computer Science and Technology, BNRist, Tsinghua University, Beijing 100084, China

²College of Information Sciences and Technology, Pennsylvania State University, University Park, PA 16802, U.S.A.

E-mail: {liangd16, guoyc15, zhangsk18}@mails.tsinghua.edu.cn; taijiang@tsinghua.edu.cn; suh972@psu.edu

Received March 28, 2020; revised April 17, 2020.

Abstract Lane detection is essential for many aspects of autonomous driving, such as lane-based navigation and high-definition (HD) map modeling. Although lane detection is challenging especially with complex road conditions, considerable progress has been witnessed in this area in the past several years. In this survey, we review recent visual-based lane detection datasets and methods. For datasets, we categorize them by annotations, provide detailed descriptions for each category, and show comparisons among them. For methods, we focus on methods based on deep learning and organize them in terms of their detection targets. Moreover, we introduce a new dataset with more detailed annotations for HD map modeling, a new direction for lane detection that is applicable to autonomous driving in complex road conditions, a deep neural network **LineNet** for lane detection, and show its application to HD map modeling.

Keywords convolutional neural network (CNN), dataset, deep learning, high-definition (HD) map, lane detection

1 Introduction

In the past decade, autonomous driving has gained much attention with the popularity of in-vehicle smart devices and the improvement of vehicle-road collaboration systems. Lane detection is a basic step in many intelligent advanced driver assistance systems (ADASs), such as a lane departure warning system, which warns drivers when vehicles deviate from their lanes. ADASs, together with other traffic information detection technologies [1–3], are becoming mature and widely integrated into vehicles, especially electric ones, and people are getting used to automatic driving. However, when tested on real roads, complex road conditions such as occlusion, lighting, among other factors, make it challenging for accurate lane detection.

Lane detection is applied in both online and offline scenarios with specific requirements for performance. In the former scenarios, such as lane-based navigation and lane departure detection, the lane detection algorithm has to be fast enough with immediate feedback

about the lane the vehicle is on. In the latter scenarios, such as HD map modeling [4–7], which is the foundation for safe automatic driving, the accuracy of lane detection results plays a key role in both localization and navigation. Based on different application scenarios, we further categorize lane detection in terms of the detection target that is focused on as shown in Fig.1.



Fig.1. Differences between ego-lane (in red), ego-road (in green and red), and all-roads (in blue, green and red).

- Ego-lane detection detects the current lane and its boundary and is mainly applied online, e.g., so that autonomous driving cars can stay in the current lane with the aid of lane departure detection.

- Ego-road lane detection detects the lane number,

Survey

Special Section of CVM 2020

This work was supported by the National Natural Science Foundation of China under Grant Nos. 61902210 and 61521002, a research grant from the Beijing Higher Institution Engineering Research Center, and the Tsinghua-Tencent Joint Laboratory for Internet Innovation Technology.

*Corresponding Author

©Institute of Computing Technology, Chinese Academy of Sciences 2020

lane marking types and the road boundary of the current road. Ego-road lane detection is also mainly applied online, e.g., so that autonomous driving cars can change their lanes and make turns.

- All-roads lane detection detects the lane markings and the road boundaries of all visible roads (including the opposite lane). All-roads lane detection is more challenging and is mainly required by offline applications, such as HD map modeling.

With the rapid development of deep neural networks, similar to other computer vision tasks, the methodology to solve the lane detection problem has been taken over by learning-based methods in recent years and the state-of-the-art results have been superior to those of the traditional non-learning methods. Readers are referred to [8, 9] for detailed reviews on traditional non-learning methods.

In this survey, we focus on learning-based lane detection methods aimed at the three aforementioned scenarios. We first introduce existing lane detection datasets proposed for training and evaluation as well as our proposed new informative dataset, named **TTLane**, for all-roads lane detection and HD map modeling in Section 2. Then in Section 3, we review recent learning-based methods in terms of the three kinds of detection targets and their network designs in detail. Later we introduce our proposed network, named **LineNet**, for more complicated road conditions and its application for HD map modeling in Section 4. Finally, we make conclusions in Section 5.

2 Datasets for Lane Detection

As for learning-based lane detection, the dataset itself is determinative. From the view of statistics, the only thing the learning-based methods do is trying to fit the distribution of the dataset. On the one hand, the dataset provides the annotated data for training and evaluating different methods; on the other hand, the quality of collected data and annotations limits the capacity of different methods. We thus compare different public datasets for lane detection in terms of their annotations and applications in this section and introduce a more detailedly annotated dataset for lane detection in complex traffic conditions.

2.1 Existing Datasets

Currently, most existing public datasets for lane detection are proposed for urban roads. The **KITTI** road [10] provides two types of annotation: road segmentation and ego-lane segmentation. The road contains the segmentation covering all lanes, while the ego-lane only labels the lane the car is currently driving on. In addition to ego-lane annotations, the **ELAS** dataset [11] also marks the lane marking types (LMTs). More than 20 different scenes (with over 15 000 frames) are included in the ELAS dataset.

The **Caltech Lanes dataset** [12] contains four video sequences (or sub-dataset) in urban environments with 1 225 images in total. **BDD100K** [13] contains two types of annotation of lane markings, which indicate whether the lane marking is parallel to the driving direction or not. Lee *et al.* proposed the **VPGNet** dataset [14], consisting of approximately 20 000 images with eight lane marking types and nine road marking types for four scenarios. Different from the previous Caltech Lanes dataset [12], all lane markings in the VPGNet dataset are annotated. Another dataset is **tuSimple** lane challenge^①, which consists of 3 626 training images and 2 782 testing images taken on highway roads. tuSimple is designed for ego-road lane detection; however, the lane marking types are not distinguished and the space between lanes is not provided. Besides, a dashed lane is annotated as solid in tuSimple. **CULane** [15] currently is the biggest dataset for multiple lanes detection. However, it is not designed for HD map modeling, for there are only annotations of the road currently being driven on and the annotations of road boundaries are missing. Table 1 summarizes the differences among the above datasets and ours in terms of annotation details.

2.2 TTLane Dataset

Existing lane detection datasets are not informative enough for the purposes of all-roads lane detection and HD map modeling. For instance, necessary road boundaries and occlusion areas for HD map modeling are not annotated in existing datasets. To this end, we introduce a new dataset^②, named TTLane, with more than 10k images where there are comprehensive annotations for all roads in different light conditions and weather conditions ranging from sunny to rainy.

^①TuSimple. TuSimple lane detection challenge. <https://github.com/TuSimple/tusimple-benchmark/tree/master/doc/lane-detection>, Apr. 2020.

^②<https://cg.cs.tsinghua.edu.cn/TTLane>, May 2020.

Table 1. Comparison of Different Lane Detection Datasets

| Dataset | Anno. Type | LMT | All Roads | Road Bound. | Occlusion | # Images |
|------------------------------|------------|-----|-----------|-------------|-----------|-------------------|
| KITTI road [10] | Seg. | No | No | No | No | 191 |
| ELAS [11] | Line | Yes | No | No | No | $\approx 15\,000$ |
| Caltech Lanes [12] | Line | Yes | No | No | No | 1 225 |
| BDD100K [13] | Line | No | Yes | Yes | No | 100 000 |
| VPGNet [14] | Line | Yes | Yes | No | No | 21 097 |
| tuSimple Lane ⁽³⁾ | Line | No | No | No | No | 6 408 |
| CULane [15] | Line | No | No | Yes | No | 133 235 |
| TTLane | Line | Yes | Yes | Yes | Yes* | 13 200 |

Note: “Seg.” is abbreviated for “segmentation”, “Anno.” for “annotation”, “Bound.” for “boundary” and “#” means “number of”. *: part (3 000 images) of TTLane are annotated with occlusions.

Annotation. To model HD maps, the dataset should offer more considerable details than any existing dataset. In our dataset, LMTs are provided and all lanes in the image are annotated. Furthermore, our LMTs are more concise, including white solid, white dash, yellow solid, yellow dash and double lines. Gaps inside dashed lines are also annotated. The differences among datasets are summarized in Table 1 and illustrated in Fig.2.

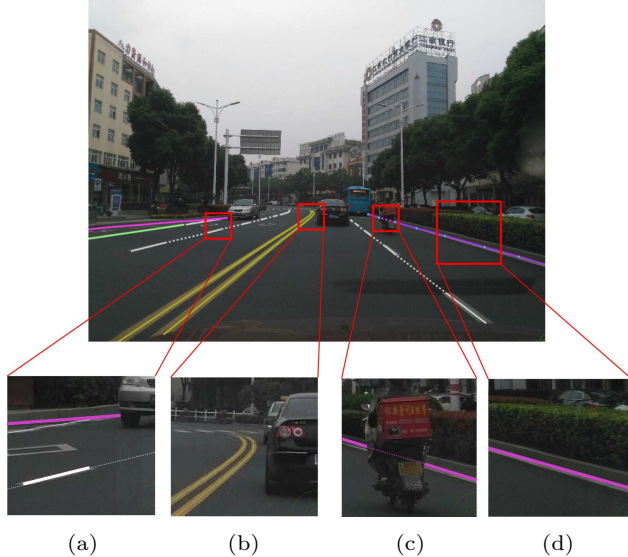


Fig.2. Annotations of our TTLane dataset. (a) Dash lanes. (b) Double lanes. (c) Occlusion segments. (d) Road boundaries.

Our dataset is the only dataset that offers annotations of road boundaries and occlusion segments. Road boundaries are necessary for many HD maps applications, and occlusion segments are useful for improving the accuracy of lane detection. Annotations of road boundaries and the separately labeled double lines make our TTLane a challenging large-scale dataset for

lane detection in urban environments.

We manually annotated the center points of lane markings, and continuous lane markings are fitted and plotted using a Bezier curve. Each lane marking is associated with a type. There are six types in total, i.e., white solid, white dash, yellow solid, yellow dash, road boundary and “other”. If there are double yellow solid lines in the center of the road, the annotator must draw two parallel yellow solid lines, as shown in Fig.2. This annotation strategy can cope with complicated double lane markings, such as a left solid lane and a right dashed lane.

Annotations of occlusion segments and gaps inside dashed lanes are among other features of our dataset. Liang et al. [16] showed that the information from occluded regions can improve image segmentation performance. Therefore, we also annotated the occlusion segments using a dotted, continuous lane. The same is true for gaps in dashed lanes. Note that we do not distinguish occlusions from gaps and annotate them with the same format. More example annotations from our dataset can be seen in Fig.3.

Statistics. TTLane consists of 13 200 images, 3 000 of which were annotated with occlusion information and the rest 10 200 images were normally annotated. Isolation belts, roadblocks and other objects that may affect the road conditions were annotated as “other”. Regarding comprehensive annotation, our dataset is the most detailed dataset for road modeling in urban environments. The details of the dataset are shown in Table 2.

3 Lane Detection with Deep Learning

With the rapid development of deep learning methods, especially the deep CNNs are also applied in the task of lane detection, achieving promising results,

⁽³⁾TuSimple. TuSimple lane detection challenge. <https://github.com/TuSimple/tusimple-benchmark/tree/master/doc/lane-detection>, Apr. 2020.

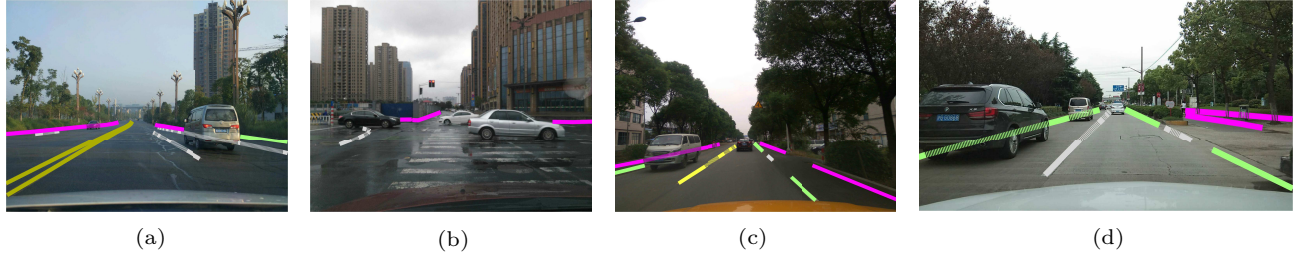


Fig.3. Gallery shows the annotations of our TTLane dataset.

Table 2. Statistics for Our TTLane Dataset

| Width (px.) | Height (px.) | Image | WS | WD | RB | YS | YD | Other | Total |
|----------------|----------------|--------|--------|--------|--------|-------|-------|-------|--------|
| 2058 ± 163 | 1490 ± 215 | 13 200 | 24 831 | 14 136 | 22 598 | 8 945 | 2 106 | 2 613 | 75 231 |

Note: px.: pixel; WS: white solid; WD: white dash; RB: road boundaries; YS: yellow solid; YD: yellow dash.

ranging from ego-lane detection, ego-road lane detection to all-roads lane detection with an increasing difficulty. In this section, we focus on recent progress of learning-based methods for the lane detection on these three aspects and analyze designs of deep neural networks. We also discuss possible trends for effective and robust lane detection in real-world road conditions.

3.1 Ego-Lane Detection

The ego-lane detection is often used in scenarios such as **lane departure warning** system (LDWS) and lane centering, where real-time performance is usually required in order to instantly determine whether a vehicle is driving normally in its lane, thus reducing traffic accidents. To this end, various features ranging from traditional hand-crafted, such as Hough^[11], to learned features^[5, 17–23] have been adopted to detect the ego-lane. Though the network details may vary a lot across different methods, they still can be roughly divided into two fashions: **single task network** and **multi-task network**. In the former case, the networks are specifically designed for the only task, i.e., lane detection; while in the latter case, other than the lane detection, the networks can perform other tasks, such as road classification, vehicle detection, and HD map parameters regression. Although the advantages of using multi-task networks are obvious, other tasks may degrade the performance of lane detection.

Single Task. Oliveira *et al.*^[17] designed a encoder-decoder network based on **VGG** for road segmentation. Liu *et al.*^[18] proposed dilated feature pyramid network (**FPN**) with feature aggregation for drivable road detection and achieved the best *F1* score on the KITTI ego-lane segmentation task. Lyu *et al.*^[22] proposed to combine CNN and **LSTM** for road segmentation,

where the feature extracted by CNN is fed to LSTM in row/column order. In order to refine the segmentation in faraway area, the center part of the image is cropped and enlarged for prediction and fused back to the full image.

Multi-Task. Chen and Chen^[20] proposed an end-to-end network, **RBNet**, for road and road boundary detection, which is implemented as a multi-task learning problem. The network exploited **Resnet50** as the feature network, followed by three task-specific sub-networks to simultaneously detect roads and road boundaries, achieving better performance than some two-stage methods. Bittel *et al.*^[5] estimated essential HD maps parameters, such as street type, the number of lanes, roadside and angle, using a multi-task CNN. These parameters are generated from separated fully-connected layers fed with shared CNN features. However, this method requires intensity map, semantic map and occupancy grid map generated from navigation as inputs. Teichmann *et al.*^[21] also presented an end-to-end multil-task architecture for simultaneous street classification, vehicle detection and road segmentation. The three decoders take the feature extracted from a shared 3-layer CNN encoder as input. The network is one-stage and achieves real-time performance.

3.2 Ego-Road Lane Detection

Different from the ego-lane detection, ego-road lane detection needs to find out all the lanes in the road of driving direction^[14, 24, 25]. Despite the common challenges met in ego-lane detection, such as light conditions, weather conditions, occlusions, and so on, the number of lanes in ego-road lane detection may change due to the varying width of roads. The ego-road lane detection is thus regarded as an instance segmentation

problem. One kind of methods is end-to-end [14, 15, 25–28] trainable, directly outputting individual lanes, and the other kind of methods [29–33] for ego-road lane detection first trains a segmentation network to locate the lane markings, and then performs post-processes, e.g., clustering and lane curve fitting, to obtain the lane instances.

End-to-End. Lee *et al.* [14] proposed a multi-task CNN to detect lanes and road marks simultaneously by **taking advantage of the vanishing point of lanes**. They achieved the best *F1* score on the **Caltech Lane** dataset [12]. Pan *et al.* [15] designed a special layer called Spatial CNN (SCNN) to segment out the road lanes. **SCNN is a special 3D manipulation that facilitates message passing along rows/columns and enlarges the receptive field to the whole image.** This is useful for lane recognition since some lanes may cross over the image. The network also learns to connect the dashed lanes for they were annotated as solid lanes in tuSimple. However, since this method treats the lane detection as a semantic segmentation task, it can only detect a predefined number of lanes in the input image. Fan *et al.* [26] proposed **SpinNet** which includes a new spinning convolution layer to gather more information from multiple directions, contributing to the whole lane boundary detection. Unlike previous methods extracting lane instances from lane segmentation, SpinNet introduces a lane boundary parameterization branch to regress lane curves from the feature map and is thus end-to-end trainable. Hou *et al.* [25] proposed a new module **Self Attention Distillation (SAD)**, for **ENet** encoder [34] to learn the self-attention between two neighboring ENet encoders and segments out the fixed number of lanes. Pizzati *et al.* [27] cascaded an instance segmentation network and a classification network to detect lanes with types. Instead of segmenting lanes, Philion [28] adapted ResNet-50 [35] to auto-regress the polyline representation of lanes and thus could detect an arbitrary number of lanes on the road.

Segmentation Plus Post-Processing. De Brabandere *et al.* [29] proposed a general network for instance segmentation which can be applied to lane detection by clustering features through a fast post-process. The network learned a map from the image space to a feature space with a discriminative loss function, which satisfies that the pixels belonging to the same instance are close in the feature space and far enough from each other otherwise. Neven *et al.* [30] proposed a complicated network consisting of a lane segmentation sub-network, a pixel embedding sub-network like in [29]

and a perspective transformation network. The lane instances are obtained using iterative clustering based on the predicted lane masks and features. Finally, a 3rd order polynomial is fitted for each lane instance in the learned perspective transformation. Hsu *et al.* [31] also exploited a segmentation network to find out the lanes and the lane features at the same time, which are required to be close enough for the same lane and far enough for different lanes. The final instance level lanes are obtained through clustering on the learned lane features in post-processing. Chang *et al.* [33] first trained a lane segmentation network on their own city road dataset collected on complicated weather conditions, and later the segmented lane markings were clustered using unsupervised attentive voting and the corresponding curves are fitted in bird's eye view.

3.3 All-Roads Lane Detection

All-roads lane detection is required for more intelligent autonomous driving in complicated road conditions, especially the crossroads, where the vehicle may take turns. In this situation, the lanes in other road should be clearly detected for the autonomous driving system to determine which lane to turn to. For HD map modeling, the lanes in all roads should also be detected and stored in the map. To detect lanes in other roads from a front-view image, some methods [11, 14, 17, 20, 21, 36, 37] aimed at ego-lane or ego-road lane detection can also be retrained on the data with all roads annotated to fulfill the task of all-roads lane detection. A large field-of-view (FoV) is important for the all-roads lane detectors to understand global structures. For example, to detect the gaps inside dashed lanes, FoV is required to be large enough to cover the length of the gap. Thus more input modalities [4, 38–42] are required through other views or specific equipment to enlarge FoV.

Front View. There are two types of approaches that can detect all road lanes from a front-view image using ego-lane or ego-road lane detectors. The first one is based on road surface segmentation aimed at ego-lane detection [17, 20, 21]. However, these methods are easily affected by occlusions; besides, the types of lane boundaries are ignored. The second type of approaches exploits the informative lane markings [11, 14, 36, 37]. However, the lane markings would become too narrow and too small to be distinguished towards the vanishing points due to the front-view input image.

More Input Modalities. He *et al.* [38] combined features from the front view and the bird's eye view for

lane detection. These two views were also exploited by Garnett *et al.*^[42] to train a two-stream and end-to-end network to predict road plane and 3D lanes. Bai *et al.*^[41] combined LiDAR and RGB camera data for lane prediction, where the 3D LiDAR points were used to predict the height and the angle of ground plane and the image was re-projected to the bird's eye view using the predicted ground plane parameters. Máttyus *et al.*^[4] used aerial images to improve the fine-grained segmentation result from the ground view, through which all roads can be recognized and modeled. Azimi *et al.*^[39] exploited the encoder-decoder architecture to semantically segment out all the lanes in remote sensing image, which is challenge due to the lack of details for covered or blurry roads. Based on this work, Kurz *et al.*^[40] reconstructed high-definition lanes using multiview aerial images.

3.4 Trends in Learning-Based Lane Detection

As we know, current ADASs serve as an assistant for the driver, and to fulfill the goal of safe and satisfying autonomous driving on real-world roads, there still remain many issues to be improved or tackled. Imagining the real-world use case, a lane detection method should still be working throughout a whole year, no matter whether it is the sunny or cloudy, the day or the night, the summer or the winter, the urban or the rural, the congested or the clear, etc. The key issue is to make the lane detection method robust as well as effective under various road conditions. The strategies to solve these issues give us some trends for developing more intelligent lane detection methods. Specifically, we discuss some trends to future lane detection methods in terms of sensor modalities, datasets and methods.

- *More Modalities.* Currently most methods are designed for RGB images; however, the appearance of the road can be changed under different light conditions, weather/season conditions, etc. More input modalities such as LiDAR points, infrared image, aerial image and panorama, can be complementary to each other and contribute to a large FOV for a better global lane detection.

- *Improving the Generality.* Constrained by existing datasets, lane detection methods trained on one dataset are probably not generalized to others. Transfer learning or a more general dataset that represents the real-world road conditions should be explored.

- *3D Lane Detection.* 2D lane detection misses the key distance information, which is essential for some actions, e.g., making turns or merging into another lane.

The 3D lane should be detected with the help of range sensors, more views or video sequences.

- *Multi-Task Networks.* An intelligent ADAS would gather all perceived traffic information, such as traffic signals, vehicles, pedestrians and traffic signs to make decisions. Computational friendly multi-task networks for simultaneous lane detection and other tasks to reduce the networks loaded for an intelligent autonomous driving system are necessary.

- *Semi-Supervised or Unsupervised Learning Methods.* For lane detection they are also preferred to relieve people from constructing a more and more comprehensive lane detection dataset with the increasing demands for complicated road scene understanding.

4 LineNet: New Solution for Accurate Lane Detection in Complex Road Conditions

Current CNN-based lane detection methods are mainly adapted from networks that are designed for image segmentation tasks, which may not be suitable for line detection and could generate inaccurate results. We propose a novel deep CNN, named LineNet, which is specially designed for accurate lane detection under complex road conditions based on our dataset.

4.1 Network Details

As illustrated in Fig.4, LineNet takes a pre-trained DeepLab^[43] as its backbone network and contains two main CNN modules: the Line Prediction (LP) layer and the Zoom module. The outputs of both CNNs are fed into the image space line cluster and produce the final results.

Line Prediction Layer. Similar to Zhu *et al.*'s three-branch prediction procedure^[1], our LP layer contains six layers, i.e., a mask layer, a position layer, a direction layer, a confidence layer, a distance layer, and a type layer, as shown in Fig.5.

Zoom Module. It focuses on areas where the results are not confident enough (less than 0.5) in low resolution images, and splits the data flow through the CNN into two streams: 1) a thumbnail CNN; 2) a high-resolution cropping CNN. Fig.6 illustrates the architecture of the Zoom module. The thumbnail CNN provides a global context for the features that the high-resolution CNN "sees" in detail. These two CNNs share weights and features. Sharing is achieved via a layer we call the "injection layer", where features are fused from both CNNs and fed into the high-resolution CNN using element-wise addition.

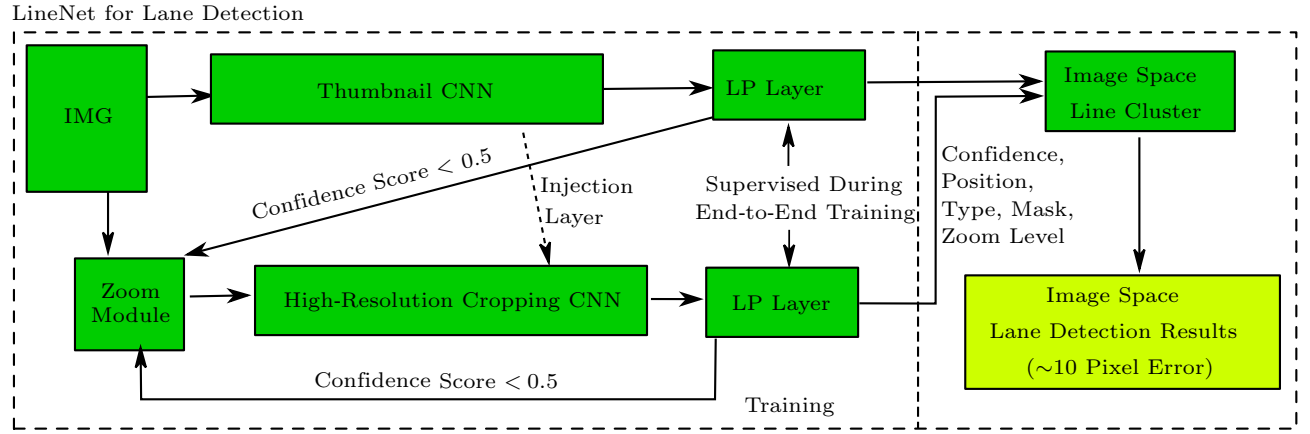


Fig.4. Overview of LineNet for lane detection. First, the input image is fed into a thumbnail CNN and the LP layer. Second, the high-resolution cropping CNN will zoom into the region where the thumbnail CNN does not have enough confidence. Finally the outputs of both CNNs are fed into the image space line cluster and produce the final results.

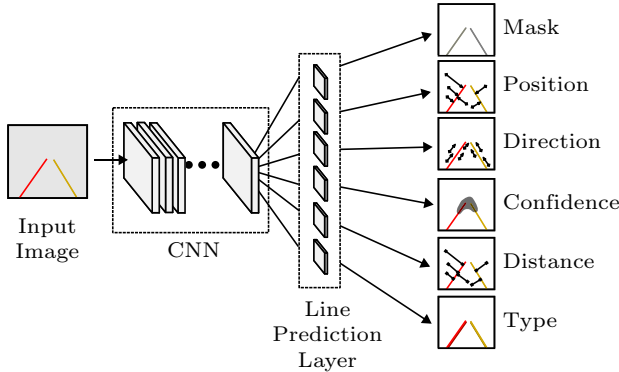


Fig.5. Illustration of the LP layer. LineNet will become confident when two lane markings are sufficiently far from each other.

Post Processing. The results that LineNet predicted were still discrete points. To achieve accurate

and smooth lines, points were clustered together using DBSCAN^[44] with our hierarchical distance (d_h) and fitted into lines. Specifically, for the image coordinate $p_i = (x, y)$ predicted from line position at zoom level z_i , the hierarchical distance between discrete points p_i and p_j is defined as $d_h(i, j) = \max(z_i, z_j) \|p_i - p_j\|_2$ to manipulate the appropriate distance from different zoom ratios. After DBSCAN^[44] clustering, line points of each cluster were fitted into a polynomial $p(x) = p_0 + p_1x + p_2x^2 + p_3x^3$, then smooth and reliable lines were achieved as the final lane detection results.

4.2 Experiments

In this subsection, we first compare our LineNet with recent lane detection methods for two common subtasks, i.e., lane detection and comprehensive lane

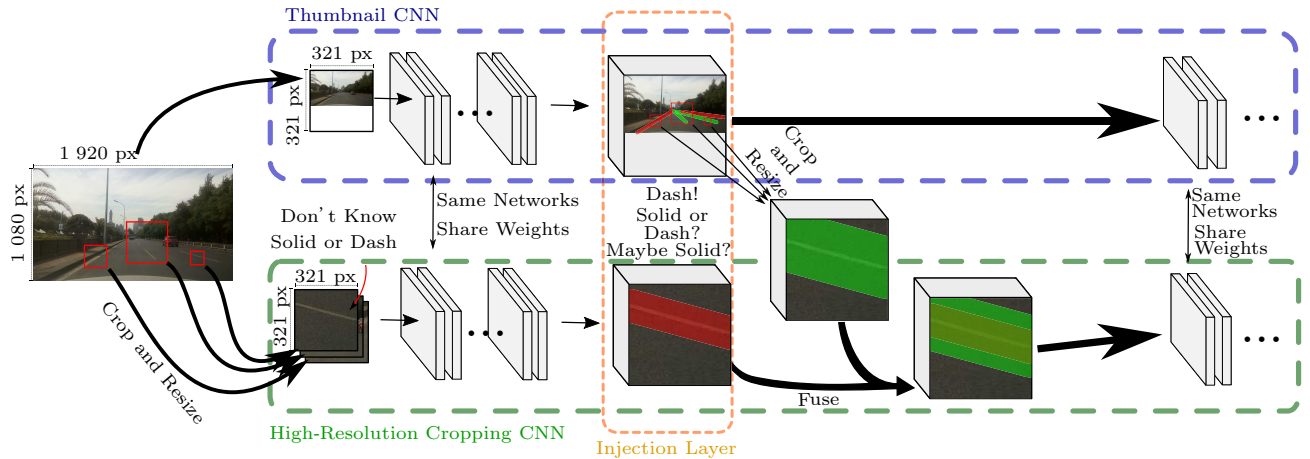


Fig.6. Zoom module fuses data from the thumbnail CNN and the high-resolution cropping CNN together, and detects a dashed lane in the high-resolution stream. The thumbnail CNN can recognize the dashed lane because it has a larger FoV, while the high-resolution CNN accurately locates the lane markings.

detection. We also conduct ablation studies to demonstrate the effectiveness of our proposed modules in LineNet.

Implementation Details. Our LineNet is implemented using the Tensorflow 1.2 framework. We set the learning rate as the base learning rate multiplying $(1 - \frac{\#iter}{MaxIter})^{power}$; the base learning rate is $2e^{-4}$, and the power (*power*) is 0.9. We use 0.9 for the momentum and $5e^{-4}$ for the weight decay. The number of training iterations (*#iter*) varies due to the sizes of datasets, but a maximum number of 80 000 iterations (*MaxIter*) are sufficient for the three datasets we evaluate on in Table 3. For the Zoom module, we use the 66th layer (4b13) of the Dilated Resnet architecture^[43] as the injection layer, and experiments show that the average fusion works well among various fusion strategies. All experiments are run on a desktop PC with an Intel Core i7-6850K CPU, NVIDIA 1080Ti GPU and 64 G RAM.

Table 3. Comparisons of Caltech, VPGNet and Ours Using the *F1* Score on Caltech Lanes Dataset

| Method | <i>F1</i> |
|-------------------------|--------------|
| Caltech ^[12] | 0.723 |
| VPGNet ^[14] | 0.866 |
| Ours | 0.955 |

Note: The number in bold indicates the best performance.

Comparison of Lane Detection. In this situation, we only evaluate the detected positions of lanes without considering their types. We perform experiments on the Caltech Lanes dataset^[12], the CULane dataset^[15] and our TTLane dataset. In the Caltech Lanes dataset, we draw the ground-truth and predicted lines with a thickness of 40 pixels and evaluate the performance using the *F1* score. We also adopt the method mentioned in SCNN^[15], which draws lane markings with width equal to 30 pixels and regards IoU (intersection over union) > 0.5 as a successful detection when computing the precision, recall and *F1* score.

We compare our method against VPGNet^[14], SCNN^[15], Mask R-CNN^[45] and MLD-CRF^[46] with available measurements and methods provided by different datasets. Results are listed in Tables 3–5, respectively. Our method achieves the best performance on all three datasets, and even exceeds the previous best performance by a significant margin on the Caltech Lanes dataset.

Comparison of Comprehensive Lane Detection. In this situation, we compare LineNet with three state-of-the-art methods (SCNN^[15], Mask R-CNN^[45] and MLD-CRF^[46]) on the two settings, i.e., ego-road and

all-roads, by taking LMT into account. Since SCNN^[15] and MLD-CRF^[46] do not predict LMT, the type information is not considered when evaluating these two methods. Results are shown in Table 6. Our method also achieves the best performance on all evaluation metrics by significant margins.

Table 4. Comparisons Between SCNN and Ours Using the *F1* Score on CULane Dataset

| Method | <i>F1</i> |
|----------------------|--------------|
| SCNN ^[15] | 0.713 |
| Ours | 0.731 |

Note: The number in bold indicates the better performance.

Table 5. Comparisons of SCNN, Mask R-CNN, MLD-CRF and Ours Using the *F1* Score, Precision (PRE.) and Recall (REC.) on TTLane Dataset

| Method | <i>F1</i> | PRE. | REC. |
|----------------------------|--------------|--------------|--------------|
| SCNN ^[15] | 0.790 | 0.794 | 0.787 |
| Mask R-CNN ^[45] | 0.708 | 0.764 | 0.660 |
| MLD-CRF ^[46] | 0.412 | 0.556 | 0.327 |
| Ours | 0.832 | 0.848 | 0.816 |

Note: The number in bold indicates the best performance.

Table 6. Comparison of Comprehensive Lane Detection on TT-Lane

| Method | Ego-Road | | | All-Roads | | |
|----------------------------|--------------|--------------|--------------|--------------|--------------|--------------|
| | <i>F1</i> | PRE. | REC. | <i>F1</i> | PRE. | REC. |
| SCNN ^[15] | 0.608 | 0.594 | 0.623 | 0.560 | 0.537 | 0.585 |
| Mask R-CNN ^[45] | 0.568 | 0.580 | 0.556 | 0.521 | 0.538 | 0.506 |
| MLD-CRF ^[46] | 0.206 | 0.260 | 0.171 | 0.193 | 0.267 | 0.150 |
| Ours | 0.708 | 0.651 | 0.778 | 0.663 | 0.613 | 0.722 |

Note: The number in bold indicates the best performance.

To intuitively demonstrate the advantages of LineNet, Fig.7 presents some prediction results from the testing set of the TTLane dataset. We can conclude from the experiment that mask-based lane detection methods, like Mask R-CNN and SCNN, cannot handle details well, such as the double line detection; non-learning based methods like MLD-CRF can hardly perform well in complex scenes. In contrast, LineNet was robust and performed well in both situations.

4.3 HD Map Modeling: An Application of LineNet

In this subsection, we present how to incorporate our proposed LineNet for lane detection into HD map modeling on a city scale with inaccurate data collected by users using crowdsourcing strategy^[47–49]. This

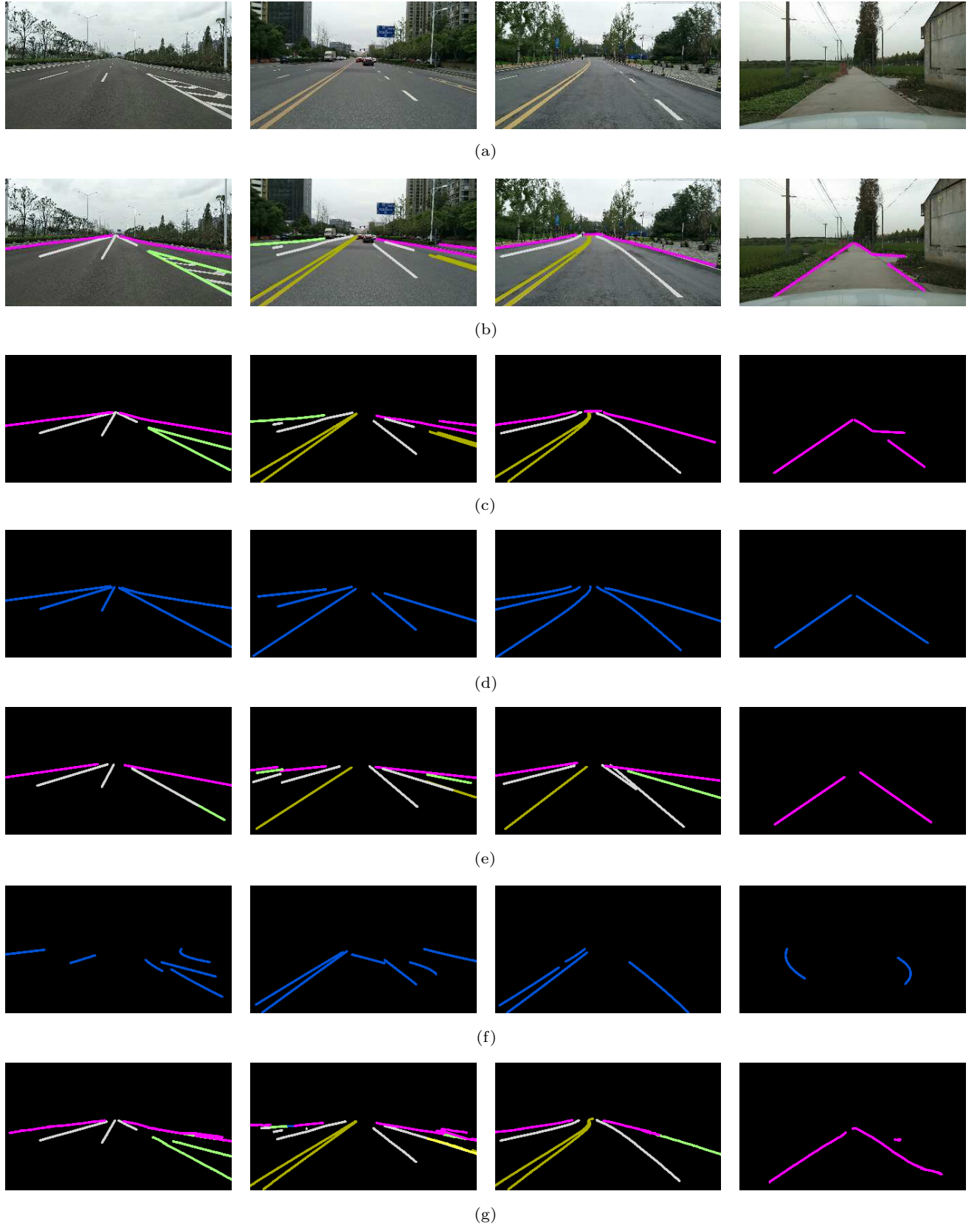


Fig.7. Visual comparisons on the TTLane testing set. (a) Original image. (b) With ground-truth lanes overlaid. (c) Ground-truth lanes. Lanes detected by (d) SCNN [15], (e) Mask R-CNN [45], (f) MLD-CRF [46], and (g) our LineNet. LineNet performs the best in detecting double lines and line direction on the remote side.

pipeline consists of OpenSfM^④, LineNet and some post-processing. In this experiment, images and GPS information were collected with three different transportation modes, i.e., cars, bicycles and electric bikes, driven by three riders to simulate the crowdsourcing on three road configurations, i.e., straight, turning, and crossroads. These riders covered different portions of the road overlapped with each other. Images were collected at an interval of [5, 20] meters, associated with inaccurate GPS information (with errors about five meters). HD maps were successfully constructed using our pipeline: the SfM stitched the parts of overlap together and the post-processing converted lane detection results to smooth and robust lines. The ground truth of these roads was also collected through high-precision LiDAR.

To further reconstruct the road surface, we segmented the point cloud obtained from SfM, and fitted all the ground point clouds to a surface with ground surface parameters (GSPs), consisting of the angle between the horizontal line of the mobile phone and the ground, and the height of the phone to the ground, for each shot position. Table 7 showed the average GSPs reconstruction error over all shots for each of the three road conditions in Fig.8.

Table 7. Performance of the Proposed HD Maps Modeling Method

| Data | Number of Shots | Height Error (m) | Rotation Error (°) | Lane Error (m) |
|-----------|-----------------|------------------|--------------------|----------------|
| Straight | 173 | 0.15 | 5 | 0.20 |
| Turning | 342 | 0.11 | 8 | 0.21 |
| Crossroad | 1476 | 0.23 | 9 | 0.31 |

The lanes that LineNet detected were still fragmented. To reconstruct the entire lanes, these detection lanes were first projected onto the road surface, and then merged using the same method introduced in Section 4. As shown in Table 7, the average lane error is just 31.3 cm, which is a significant improvement since the GPS error of our mobile devices is about 5 meters.

5 Conclusions

In this survey, we reviewed the development of datasets and applications for lane detection, summarized deep learning methods for lane detection, discussed trends for effective and robust lane detection and made improvements by introducing a new dataset with

detailed annotations and a novel deep neural network for lane detection that is more robust in complex road conditions. Meanwhile, we incorporated the proposed accurate lane detection into a new direction: HD map modeling. For the first time, we proposed a pipeline to model HD maps with crowdsourced data. Our method can reconstruct HD maps of high precision even with inaccurate data. The method also showed the ability to model HD maps accurately without special equipment, making it possible to enlarge the coverage area of HD maps efficiently. We hope this new dataset^⑤ and method can contribute to future research on HD map modeling for intelligent autonomous driving.

References

- [1] Zhu Z, Liang D, Zhang S, Huang X, Li B, Hu S. Traffic-sign detection and classification in the wild. In *Proc. the 2016 IEEE Conference on Computer Vision and Pattern Recognition*, June 2016, pp.2110-2118.
- [2] Lu Y, Lu J, Zhang S, Hall P. Traffic signal detection and classification in street views using an attention model. *Computational Visual Media*, 2018, 4(3): 253-266.
- [3] Song Y, Fan R, Huang S, Zhu Z, Tong R. A three-stage real-time detector for traffic signs in large panoramas. *Computational Visual Media*, 2019, 5(4): 403-416.
- [4] Máttyus G, Wang S, Fidler S, Urtasun R. HD maps: Fine-grained road segmentation by parsing ground and aerial images. In *Proc. the 2016 IEEE Conference on Computer Vision and Pattern Recognition*, June 2016, pp.3611-3619.
- [5] Bittel S, Rehfeld T, Weber M, Zöllner J M. Estimating high definition map parameters with convolutional neural networks. In *Proc. the 2017 IEEE International Conference on Systems, Man, and Cybernetics*, October 2017, pp.52-56.
- [6] Zang A, Xu R, Li Z, Doria D. Lane boundary extraction from satellite imagery. In *Proc. the 1st ACM SIGSPATIAL Workshop on High-Precision Maps and Intelligent Applications for Autonomous Vehicles*, November 2017, Article No. 1.
- [7] Yuan J Z, Chen H, Zhao B, Xu Y. Estimation of vehicle pose and position with monocular camera at urban road intersections. *Journal of Computer Science and Technology*, 2017, 32(6): 1150-1161.
- [8] Yenikaya S, Yenikaya G, Düven E. Keeping the vehicle on the road: A survey on on-road lane detection systems. *ACM Computing Surveys*, 2013, 46(1): Article No. 2.
- [9] Bar-Hillel A, Lerner R, Levi D, Raz G. Recent progress in road and lane detection: A survey. *Machine Vision and Applications*, 2014, 25(3): 727-745.
- [10] Fritsch J, Kühnl T, Geiger A. A new performance measure and evaluation benchmark for road detection algorithms. In *Proc. the 16th International IEEE Conference on Intelligent Transportation Systems*, October 2013, pp.1693-1700.

^④Open source structure from motion pipeline. <https://github.com/mapillary/OpenSfM>, Apr. 2020.

^⑤<https://cg.cs.tsinghua.edu.cn/TTLane>, May 2020.

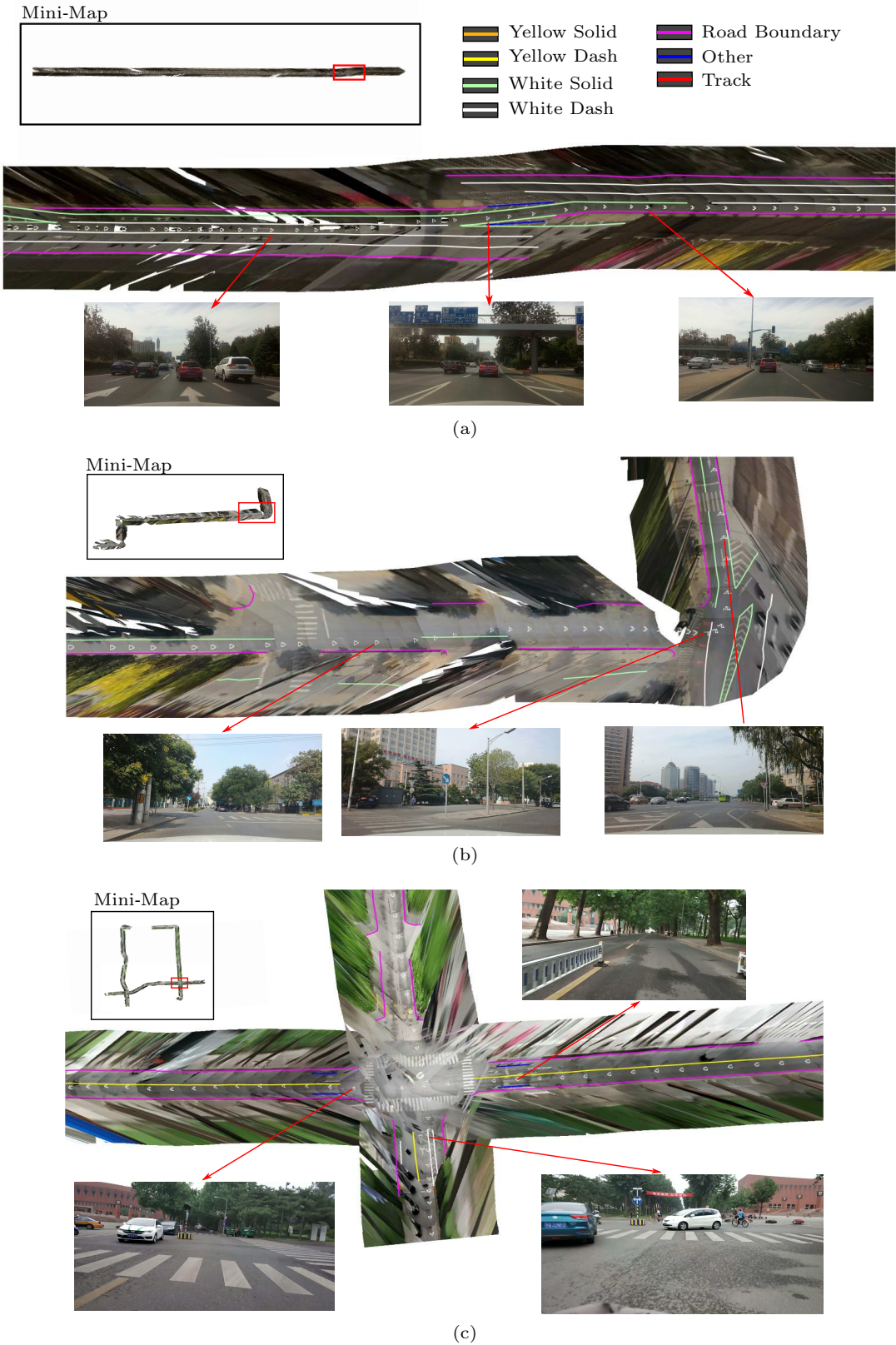
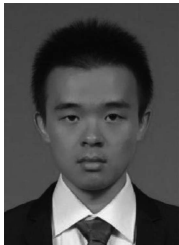


Fig.8. HD map modeling on three common road conditions: (a) straight road; (b) turning road; (c) crossing. Each sub-figure contains a mini-map on the upper left corner and a zoomed-in map, indicated by the red box in the mini-map. In the zoomed-in area, the road modeling results are shown with colored lines. Each white triangle on the road represents a shot position and the interval between two shots is about 5–20 meters. Note that we do not use any additional data (such as satellite images) except the images and GPS, and the ground surface images are stitched together from crowdsourced data.

- [11] Berriel R F, de Aguiar E, de Souza A F, Oliveira-Santos T. Ego-Lane Analysis System (ELAS): Dataset and algorithms. *Image and Vision Computing*, 2017, 68: 64-75.
- [12] Aly M. Real time detection of lane markers in urban streets. In *Proc. the 2008 IEEE Intelligent Vehicles Symposium*, June 2008, pp.7-12.
- [13] Yu F, Chen H, Wang X, Xian W, Chen Y, Liu F, Madhavan V, Darrell T. BDD100K: A diverse driving dataset for heterogeneous multitask learning. In *Proc. the IEEE Conference on Computer Vision and Pattern Recognition*, 2020. (Accepted)
- [14] Lee S, Kim J, Yoon J S, Shin S, Bailo O, Kim N, Lee T, Hong H S, Han S, Kweon I S. VPGNet: Vanishing point guided network for lane and road marking detection and recognition. In *Proc. the 2017 IEEE International Conference on Computer Vision*, October 2017, pp.1965-1973.
- [15] Pan X, Shi J, Luo P, Wang X, Tang X. Spatial as deep: Spatial CNN for traffic scene understanding. In *Proc. the 32nd AAAI Conference on Artificial Intelligence*, February 2018, pp.7276-7283.
- [16] Liang X, Wei Y, Shen X, Jie Z, Feng J, Lin L, Yan S. Reversible recursive instance-level object segmentation. In *Proc. the 2016 IEEE Conference on Computer Vision and Pattern Recognition*, June 2016, pp.633-641.
- [17] Oliveira G L, Burgard W, Brox T. Efficient deep models for monocular road segmentation. In *Proc. the 2016 IEEE/RSJ International Conference on Intelligent Robots and Systems*, October 2016, pp.4885-4891.
- [18] Liu X, Deng Z, Yang G. Drivable road detection based on dilated FPN with feature aggregation. In *Proc. the 29th IEEE International Conference on Tools with Artificial Intelligence*, November 2017, pp.1128-1134.
- [19] Kim J, Park C. End-to-end ego lane estimation based on sequential transfer learning for self-driving cars. In *Proc. the 2017 IEEE Conference on Computer Vision and Pattern Recognition Workshops*, July 2017, pp.1194-1202.
- [20] Chen Z, Chen Z. RBNNet: A deep neural network for unified road and road boundary detection. In *Proc. the 24th International Conference on Neural Information Processing*, November 2017, pp.677-687.
- [21] Teichmann M, Weber M, Zöllner J M, Cipolla R, Urtasun R. MultiNet: Real-time joint semantic reasoning for autonomous driving. In *Proc. the 2018 IEEE Intelligent Vehicles Symposium*, June 2018, pp.1013-1020.
- [22] Lyu Y, Bai L, Huang X. Road segmentation using CNN and distributed LSTM. In *Proc. the IEEE International Symposium on Circuits and Systems*, May 2019.
- [23] Mamidala R S, Uthkota U, Shankar M B, Antony A J, Narasimhadhan A V. Dynamic approach for lane detection using Google street view and CNN. In *Proc. the 2019 IEEE Region 10 Conference*, October 2019, pp.2454-2459.
- [24] Li J, Mei X, Prokhorov D V, Tao D. Deep neural network for structural prediction and lane detection in traffic scene. *IEEE Transactions on Neural Networks and Learning Systems*, 2017, 28(3): 690-703.
- [25] Hou Y, Ma Z, Liu C, Loy C C. Learning lightweight lane detection CNNs by self attention distillation. In *Proc. the 2019 IEEE/CVF International Conference on Computer Vision*, October 2019, pp.1013-1021.
- [26] Fan R, Wang X, Hou Q, Liu H, Mu T J. SpinNet: Spinning convolutional network for lane boundary detection. *Computational Visual Media*, 2019, 5(4): 417-428.
- [27] Pizzati F, Allodi M, Barrera A, García F. Lane detection and classification using cascaded CNNs. arXiv:1907.01294, 2019. <https://arxiv.org/abs/1907.01294>, March 2020.
- [28] Philion J. FastDraw: Addressing the long tail of lane detection by adapting a sequential prediction network. In *Proc. the IEEE Conference on Computer Vision and Pattern Recognition*, June 2019, pp.11582-11591.
- [29] De Brabandere B D, Neven D, Gool L V. Semantic instance segmentation with a discriminative loss function. In *Proc. the 2017 IEEE Conference on Computer Vision and Pattern Recognition Workshops*, July 2017.
- [30] Neven D, De Brabandere B, Georgoulis S, Proesmans M, Gool L V. Towards end-to-end lane detection: An instance segmentation approach. In *Proc. the 2018 IEEE Intelligent Vehicles Symposium*, June 2018, pp.286-291.
- [31] Hsu Y, Xu Z, Kira Z, Huang J. Learning to cluster for proposal-free instance segmentation. In *Proc. the 2018 International Joint Conference on Neural Networks*, July 2018.
- [32] Chen P, Lo S, Hang H, Chan S, Lin J. Efficient road lane marking detection with deep learning. In *Proc. the 23rd IEEE International Conference on Digital Signal Processing*, November 2018.
- [33] Chang D, Chirakkal V V, Goswami S, Hasan M, Jung T, Kang J, Kee S, Lee D, Singh A P. Multi-lane detection using instance segmentation and attentive voting. In *Proc. the 19th International Conference on Control, Automation and Systems*, October 2019, pp. 1538-1542.
- [34] Paszke A, Chaurasia A, Kim S, Culurciello E. ENet: A deep neural network architecture for real-time semantic segmentation. arXiv:1606.02147, 2016. <http://arxiv.org/abs/1606.02147>, March 2020.
- [35] He K, Zhang X, Ren S, Sun J. Deep residual learning for image recognition. In *Proc. the 2016 IEEE Conference on Computer Vision and Pattern Recognition*, June 2016, pp.770-778.
- [36] Jung H, Min J, Kim J. An efficient lane detection algorithm for lane departure detection. In *Proc. the 2013 IEEE Intelligent Vehicles Symposium*, June 2013, pp.976-981.
- [37] Beyeler M, Mirus F, Verl A. Vision-based robust road lane detection in urban environments. In *Proc. the 2014 IEEE International Conference on Robotics and Automation*, May 2014, pp.4920-4925.
- [38] He B, Ai R, Yan Y, Lang X. Accurate and robust lane detection based on dual-view convolutional neural network. In *Proc. the 2016 IEEE Intelligent Vehicles Symposium*, June 2016, pp.1041-1046.
- [39] Azimi S M, Fischer P, Körner M, Reinartz P. Aerial laneNet: Lane-marking semantic segmentation in aerial imagery using wavelet-enhanced cost-sensitive symmetric fully convolutional neural networks. *IEEE Transactions on Geoscience and Remote Sensing*, 2019, 57(5): 2920-2938.
- [40] Kurz F, Azimi S M, Sheu C, d'Angelo P. Deep learning segmentation and 3D reconstruction of road markings using multiview aerial imagery. *ISPRS International Journal of Geo-Information*, 2019, 8(1): Article No. 47.

- [41] Bai M, Mátyus G, Homayounfar N, Wang S, Lakshmikanth S K, Urtasun R. Deep multi-sensor lane detection. In *Proc. the 2018 IEEE/RSJ International Conference on Intelligent Robots and Systems*, October 2018, pp.3102-3109.
- [42] Garnett N, Cohen R, Pe'er T, Lahav R, Levi D. 3D-laneNet: End-to-end 3D multiple lane detection. In *Proc. the 2019 IEEE/CVF International Conference on Computer Vision*, October 2019, pp.2921-2930.
- [43] Chen L, Papandreou G, Kokkinos I, Murphy K, Yuille A L. DeepLab: Semantic image segmentation with deep convolutional nets, Atrous convolution, and fully connected CRFs. *IEEE Transactions on Pattern Analysis and Machine Intelligence*, 2018, 40(4): 834-848.
- [44] Ester M, Kriegel H, Sander J, Xu X. A density-based algorithm for discovering clusters in large spatial databases with noise. In *Proc. the 2nd International Conference on Knowledge Discovery and Data Mining*, August 1996, pp. 226-231.
- [45] He K, Gkioxari G, Dollár P, Girshick R B. Mask R-CNN. *IEEE Transactions on Pattern Analysis and Machine Intelligence*, 2020, 42(2): 386-397.
- [46] Hur J, Kang S, Seo S. Multi-lane detection in urban driving environments using conditional random fields. In *Proc. the 2013 IEEE Intelligent Vehicles Symposium*, June 2013, pp.1297-1302.
- [47] Chen P, Sun H, Fang Y, Huai J. Collusion-proof result inference in crowdsourcing. *Journal of Computer Science and Technology*, 2018, 33(2): 351-365.
- [48] Zhang A, Li J, Gao H, Chen Y, Ma H, Bah M J. CrowdDOLA: Online aggregation on duplicate data powered by crowdsourcing. *Journal of Computer Science and Technology*, 2018, 33(2): 366-379.
- [49] Mendiboure L, Chalouf M A, Krief F. Edge computing based applications in vehicular environments: Comparative study and main issues. *Journal of Computer Science and Technology*, 2019, 34(4): 869-886.



Dun Liang is a Ph.D. candidate in the Department of Computer Science and Technology at Tsinghua University, Beijing, where he received his B.S. degree in computer science and technology, in 2016. His research interests include computer graphics, visual media and high-performance computing.



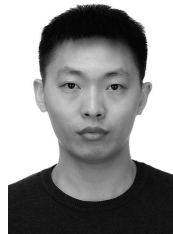
computer vision.

Yuan-Chen Guo received his B.S. degree in computer science and technology from Tsinghua University, Beijing, in 2019, where he is currently pursuing his Ph.D. degree in the Department of Computer Science and Technology of the same university. His research interests include computer graphics and



media analysis, and computer vision.

Shao-Kui Zhang is currently a Ph.D. candidate in the Department of Computer Science and Technology at Tsinghua University, Beijing. He received his B.S. degree in software engineering from Northeastern University, Shenyang, in 2018. His research interests include computer graphics,



learning, SLAM and human robot interaction.

Tai-Jiang Mu is currently an assistant researcher in the Department of Computer Science and Technology, Tsinghua University, Beijing, where he received his B.S. and Ph.D. degrees in computer science and technology in 2011 and 2016, respectively. His research interests include visual media



Xiaolei Huang received her B.E. degree in computer science from Tsinghua University, Beijing, in 1999, and her M.S. and Ph.D. degrees in computer science from Rutgers University, NJ, in 2001 and 2006, respectively. She is currently an associate professor in the College of Information Sciences and Technology at the Pennsylvania State University, University Park, PA. Her research interests are in the areas of biomedical image analysis, computer vision, and machine learning, focusing on methods for object recognition, image segmentation, image synthesis, registration/matching, tracking, skeletonization, and computer-assisted diagnosis and intervention.

JOURNAL OF COMPUTER SCIENCE AND TECHNOLOGY

Volume 35, Number 3, May 2020

Special Section of CVM 2020

| | |
|---|--|
| Preface | <i>Shi-Min Hu, Ying He, and Belen Masia (491)</i> |
| Lane Detection: A Survey with New Results | <i>Dun Liang, Yuan-Chen Guo, Shao-Kui Zhang, Tai-Jiang Mu, and Xiaolei Huang (493)</i> |
| Denoising Stochastic Progressive Photon Mapping Renderings Using a Multi-Residual Network | <i>Zheng Zeng, Lu Wang, Bei-Bei Wang, Chun-Meng Kang, and Yan-Ning Xu (506)</i> |
| A Comprehensive Pipeline for Complex Text-to-Image Synthesis | <i>Fei Fang, Fei Luo, Hong-Pan Zhang, Hua-Jian Zhou, Alix L.H. Chow, and Chun-Xia Xiao (522)</i> |
| Two-Stream Temporal Convolutional Networks for Skeleton-Based Human Action Recognition | <i>Jin-Gong Jia, Yuan-Feng Zhou, Xing-Wei Hao, Feng Li, Christian Desrosiers, and Cai-Ming Zhang (538)</i> |
| Reference Image Guided Super-Resolution via Progressive Channel Attention Networks | <i>Huan-Jing Yue, Sheng Shen, Jing-Yu Yang, Hao-Feng Hu, and Yan-Fang Chen (551)</i> |
| Automatic Video Segmentation Based on Information Centroid and Optimized SaliencyCut | <i>Hui-Si Wu, Meng-Shu Liu, Lu-Lu Yin, Ping Li, Zhen-Kun Wen, and Hon-Cheng Wong (564)</i> |
| EmotionMap: Visual Analysis of Video Emotional Content on a Map | <i>Cui-Xia Ma, Jian-Cheng Song, Qian Zhu, Kevin Maher, Ze-Yuan Huang, and Hong-An Wang (576)</i> |

Artificial Intelligence and Pattern Recognition

| | |
|--|---|
| Distinguishing Computer-Generated Images from Natural Images Using Channel and Pixel Correlation | <i>Rui-Song Zhang, Wei-Ze Quan, Lu-Bin Fan, Li-Ming Hu, and Dong-Ming Yan (592)</i> |
| Next POI Recommendation Based on Location Interest Mining with Recurrent Neural Networks | <i>Ming Chen, Wen-Zhong Li, Lin Qian, Sang-Lu Lu, and Dao-Xu Chen (603)</i> |
| Word-Pair Relevance Modeling with Multi-View Neural Attention Mechanism for Sentence Alignment | <i>Ying Ding, Jun-Hui Li, Zheng-Xian Gong, and Guo-Dong Zhou (617)</i> |

Computer Networks and Distributed Computing

| | |
|--|---|
| Cloaking Region Based Passenger Privacy Protection in Ride-Hailing Systems | <i>Yubin Duan, Guo-Ju Gao, Ming-Jun Xiao, and Jie Wu (629)</i> |
| Deploy Efficiency Driven k -Barrier Construction Scheme Based on Target Circle in Directional Sensor Network | <i>Xing-Gang Fan, Zhi-Cong Che, Feng-Dan Hu, Tao Liu, Jin-Shan Xu, and Xiao-Long Zhou (647)</i> |

Survey

| | |
|--|--|
| Data-Driven Approaches for Spatio-Temporal Analysis: A Survey of the State-of-the-Arts | <i>Monidipa Das and Soumya K. Ghosh (665)</i> |
| A Survey on Performance Optimization of High-Level Synthesis Tools | <i>Lan Huang, Da-Lin Li, Kang-Ping Wang, Teng Gao, and Adriano Tavares (697)</i> |

JOURNAL OF COMPUTER SCIENCE AND TECHNOLOGY 《计算机科学技术学报》

Volume 35 Number 3 2020 (Bimonthly, Started in 1986)

Indexed in: SCIE, Ei, INSPEC, JST, AJ, MR, CA, DBLP

Edited by:

THE EDITORIAL BOARD OF JOURNAL OF COMPUTER SCIENCE AND TECHNOLOGY

Zhi-Wei Xu, Editor-in-Chief, P.O. Box 2704, Beijing 100190, P.R. China

Managing Editor: Feng-Di Shu E-mail: jcst@ict.ac.cn http://jcst.ict.ac.cn Tel.: 86-10-62610746

Copyright ©Institute of Computing Technology, Chinese Academy of Sciences 2020
Sponsored by: Institute of Computing Technology, CAS & China Computer Federation

Supervised by: Chinese Academy of Sciences
Undertaken by: Institute of Computing Technology, CAS

Published by: Science Press, Beijing, China

Printed by: Beijing Kexin Printing House

Distributed by:

China: All Local Post Offices

Other Countries: Springer Nature Customer Service Center GmbH, Tiergartenstr. 15, 69121 Heidelberg, Germany

Available Online: <https://link.springer.com/journal/11390>

